POLITECNICO
MILANO 1863

SCUOLA DI INGEGNERIA INDUSTRIALE
E DELL'INFORMAZIONE

Executive Summary of the Thesis

LES Simulation of Calcium Hydroxide discharge for Ocean Liming with coal carriers

Laurea Magistrale in Aeronautical Engineering - Ingegneria Aeronautica

Author: Diego Bindoni

Advisor: Prof. Antonella Abbà

Academic year: 2022-2023

1. Introduction

On both broad and local sizes, the consequences of pollution from human activities on the environment are observable and quantifiable (Bindoff et al. [2]), including glaciers melting, microplastics in food, and air pollution in big cities. The acidity of the seas as a result of higher amounts of CO_2 in the atmosphere is a phenomenon that is less well-known to the general population. In reality, the sea absorbs a sizable amount of the available CO_2, which breaks down into bicarbonate, carbonate, and H^+ ions, lowering the pH. Several marine species at the base of the food chain, like plankton, mollusks, and corals, are seriously threatened by the degrowth in pH because it prevents the synthesis of calcium carbonate. The scientific community has examined the issue, and a number of technologies and strategies are still being researched and developed to help stop the acidification of the oceans. The so-called *Ocean Liming*, which entails releasing alkaline materials into the ocean to raise the pH and the capacity of CO_2 absorption (Kheshgi [6]), is one of the potential approaches on which the current thesis is founded. In the present work *Calcium Hydroxide* ($CaOH_2$), also called *slurry* or *slaked lime*, is discharged in the wake of a KRISO ship, following preliminary investigation by [3]. LES simulations have been performed using the OpenFOAM's solver *reactingFoam*, both non-reactive and reactive, in order to appreciate the differences generated by chemical reactions. Simulations were carried out for three cases of initial concentration:

- 2 g/l which is a low concentration case and presumably low risk that requires a lot of water, as visible from table **??**;
- 20 g/l which is a limit for the chemistry model adopted, since it represents the saturation limit of the solution. After this threshold, the slaked lime should be modeled as a particulate matter, thus requiring a lagrangian simulation, a much more expensive simulation that takes into account drag effects, interactions of particles with the fluid, evaporation...;
- 86.5 g/l which is the concentration adopted in Caserini's work [3]. The hypothesis of this test, based on the statements made above, are not completely satisfied, but a comparison seemed necessary.

2. Geometry and mesh

The domain adopted for the simulations includes:

- the final portion of the hull of the ship, since the prow poorly contributes to the ship's wake, thus increasing the computational cost without providing any improvement;
- the propeller, model KP505 [7], designed by the Korea Research Institute of Ships and Ocean Engineering. Nominal diameter $D = 7.9\ m$;
- the inlet from which the slaked lime is injected, placed behind the propeller, with a diameter of $D_{inlet} = 40\ cm$;
- boundaries of the domain with dimensions referred as multiple of the propeller's diameter. The inlet section measures six diameters in width by four in height, while the length is eleven diameters;
- a refinement region for better capturing wake's fluid dynamic behaviour;
- an additional patch, called *sphereEX*, working both as a refinement region and as a faceZone for OpenFOAM, required for the simulation of the propeller's motion through the Multiple Reference Frame approach, explained in section 3. This cylinder has a diameter of 6/5 the propeller's diameter and about 3/5 D of depth.

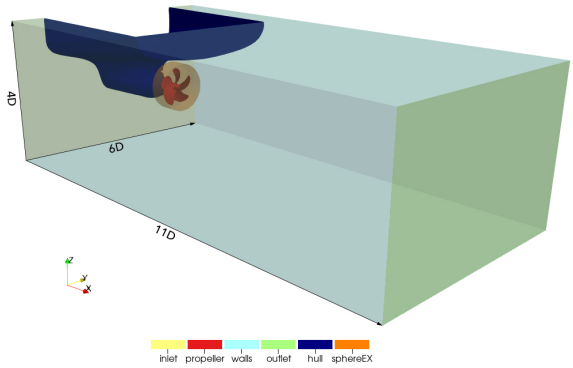

Figure 1: Domain simulated. Dimensions can be seen referred as multiple of diameters.

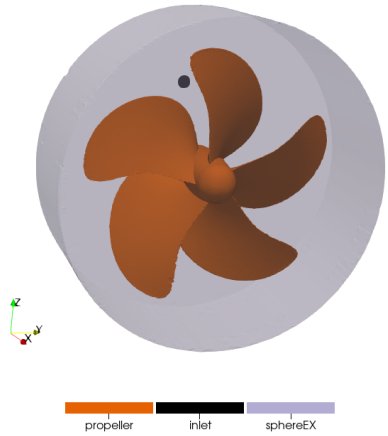

Figure 2: Propeller model with *sphereEX* and inlet.

The cruise velocity V_c of the container ship has been set to $8m/s$. In order to compute the rotational speed of the propeller n the advance ratio J is adopted. From open water characteristics and in accordance with Argentieri's thesis [4], J can be set to 0.7. From the definition of J:

$$J = \frac{V_c}{n \cdot D} \tag{1}$$

with D diameter of the propeller. By inverting the formula the rotational speed can be retrieved, obtaining a value of $n = 1.44\ Hz = 9\ rad/s$.

3. Governing equations and models adopted

The present problem requires the solution of system of partially differential equation, i.e. the Navier Stokes Equations.
Continuity equation:

$$\frac{\partial u_i}{\partial x_i} = 0 \tag{2}$$

Momentum equation:

$$\frac{\partial u_i}{\partial t} + \frac{\partial}{\partial x_i}(u_i u_j) = -\frac{1}{\rho}\frac{\partial p}{\partial x_i} + \nu \frac{\partial}{\partial x_i}(\frac{\partial u_i}{\partial x_j} + \frac{\partial u_j}{\partial x_i}) \tag{3}$$

where u_i is one of the three component of the velocity vector $\mathbf{u}$, while x_i a component of the coordinate vector $\mathbf{x}$. The kinematic viscosity is represented by ν, p is the pressure and ρ the density of the fluid.

Starting from the general formulation for an incompressible, Newtonian fluid, different models have to be adopted in order to simulate and close the whole problem. Turbulence has been modeled with a Large Eddy Simulation approach. The mesh motion is simulated with a Multiple Reference Frame model (MRF). For the chemistry, a Partially Stirred Reactor model (PaSR) is implemented in the code. A brief overview of these three strategies will be presented in the next sections.

3.1. Large Eddy Simulation

Solving the unsteady Navier-Stokes equations implies that we must take into account all the space-time scales of the solution if we want to have a result of maximum quality. With current computational resources, this is an unreachable goal for problems with very high Reynolds number like in the present work. Given these premises, LES simulations represent a good trade-off between accuracy of the solution and relatively low computational cost. First, the NS equations are decomposed in large and small-scale components and then filtered (in physical or spectral domain). Once defined the filter adopted, which in the present work is a box filter, this has to be applied to NS equations.

$$\frac{\partial \overline{u_j}}{\partial t} + \frac{\partial}{\partial x_j}(\overline{u_i u_j}) = -\frac{1}{\rho}\frac{\partial \overline{p}}{\partial x_i} + \nu \frac{\partial^2 \overline{u_j}}{\partial x_i \partial x_j}, \quad (4)$$

The filtered momentum equation can be solved using Germano Decomposition [5], where the term $\overline{u_i u_j}$ can be decomposed as:

$$\overline{u_i u_j} = \tau_{ij}^R + \overline{u}_i \overline{u}_j \quad (5)$$

The term τ_{ij}^R is called tensor of residual stresses, which can be further broken down into:

$$\tau_{ij}^R = \tau_{ij}^r + \frac{2}{3} k^R \delta_{ij} \quad (6)$$

with δ_{ij} being the Kronecker's delta and k^R the kinetic energy of residual motions, which can be included into pressure, given the fact this is an isotropic term. The anisotropic component of the residual stresses tensor τ_{ij}^r is the element that gives rise to the closure problem. This term is modeled, in this project, with the Smagorinksy Model [8]:

$$\tau_{ij}^r = -2\nu_{sgs}\overline{S}_{ij}, \quad where \quad (7)$$

$$\overline{S}_{ij} = \frac{1}{2}\left(\frac{\partial \overline{u}_i}{\partial x_j} + \frac{\partial \overline{u}_j}{\partial x_i}\right) \quad (8)$$

with $\overline{S}_{ij}$ defined as the strain rate tensor.

3.2. Multiple Reference Frame

The MRF approach will be adopted for this project, because it comes with different advantages. In order to solve the problem, it's necessary to add source terms to momentum equation (3). By defining a second reference frame inside *sphereEX*, the source terms are solved using a stationary model, thus significantly reducing the computational cost. In a nutshell, referring to a reference system which moves along with the propeller's blade, a global velocity $\boldsymbol{U}$ and an inertial velocity $\boldsymbol{U_r}$ are defined, together with a rotation vector $\boldsymbol{\Omega}$, depicting a velocity triangle.

$$\boldsymbol{U} = \boldsymbol{U_r} + \boldsymbol{\Omega} \times \boldsymbol{r} \quad (9)$$

where $\boldsymbol{r}$ is the distance from the rotation axis. From eq (9), steady Navier-Stokes equations can be rearranged with the new formulation of the global velocity, thus obtaining:

$$\underbrace{\nabla \cdot (\boldsymbol{U}\boldsymbol{U_r})}_{\text{convection term}} = -\nabla p + \nabla \cdot (\nu \nabla \boldsymbol{U}) - \underbrace{\boldsymbol{\Omega} \times \boldsymbol{U}}_{\text{source term}} \quad (10)$$

The main problem now is the convective term, which contains both the global velocity and the relative one. In a finite volume workframe, this means that the face volume flux contains the $\boldsymbol{U_r}$ too. By substituting again $\boldsymbol{U_r}$ with eq (9), a second source term can be obtained, representing a **face** (or volume) **flux correction**. This is evaluated for all the faces in the rotating zone.

3.3. Chemistry modeling

The chemical reaction between slaked lime, carbon dioxide and seawater is:

$$Ca(OH)_2 \leftrightarrow Ca^{2+} + 2OH^- \quad (11)$$

$$CO_2 + OH^- \leftrightarrow HCO_3^- \quad (12)$$

In this project, however, for comparisons with past works (Caserini [3], Abbate and Bianchi [1]), and for computational costs, only the dissolution of the slaked lime will be simulated, thus neglecting the whole carbon cycle. In the

present work the Penner's formalism will be adopted, expressing a generic chemical equations between species A, B, C as:

$$A + B \leftrightarrow C \tag{13}$$

$$\sum_{i=0}^{n} \nu_i' M_i \leftrightarrow \sum_{i=0}^{n} \nu_i'' M_i \tag{14}$$

where ν_i is the i^{th} stoichiometric coefficient respectively for reactants (ν_i') and products (ν_i'') and M_i is the i^{th} chemical specie of mixture. The evolution over time of the concentration of quantities $[A]$, $[B]$ can be described by the following equations:

$$\frac{d[A]}{dt} = \frac{d[B]}{dt} = -k_1[A][B] \tag{15}$$

$$\frac{d[C]}{dt} = k_1[A][B] \tag{16}$$

where k_1 is the rate constant that describes how fast is the production of chemical products, defined in this work with the Arrhenius law, that express the rate constant as a function of temperature only. Chemistry is related to equations (2) and (3) through source terms that can alter the composition of the fluid or the velocity field. In this project, the remarkable influences brought to the fluid-dynamics can be found mainly in the continuity equation. The energy equation, for the sake of clarity, won't be shown given the low contribution to the reaction and the project's lack of interest in investigating thermodynamic quantities. The single specie mass conservation equation is expressed as:

$$\frac{\partial \rho Y_k}{\partial t} + \frac{\partial}{\partial x_i}(\rho(u_i + V_{k,i})Y_k) = \dot{\omega}_k \ for \ k = 1, N \tag{17}$$

where $V_{k,i}$ is the i-component of the diffusion velocity V_k of species k and $\dot{\omega}_k$ is the reaction rate of species k. By definition:

$$\sum_{k=1}^{N} Y_k V_{k,i} = 0 \ and \ \sum_{k=1}^{N} \dot{\omega}_k = 0 \tag{18}$$

At this point, two contributes must be defined:

- the diffusion velocities, which are modeled with the Fick's law in this project. The approximation fixes the diffusion coefficient D required for the computation of diffusion velocities. The equation can be expressed like:
$$V_k = -D\nabla Y_k \tag{19}$$
- the source term $\dot{\omega}_k$, which is related to the specific rate k via:
$$\dot{\omega} = k\Pi_{i=1}^{N}[M_i]^{\nu_i'} \tag{20}$$

In order to take into account also mixing and turbulent effects, a finite-rate chemistry model has to be adopted. In this project, the Partially Stirred Reactor model (PaSR), will be implemented for the simulations.
With this model, the reaction rate is corrected by the chemistry solver with a reaction limiter k:

$$R_i = k\dot{\omega}_{i,chem} \tag{21}$$

The reaction limiter is computed based on the mixing time scale:

$$\tau_k = C_{mix}\sqrt{\frac{\nu}{\epsilon}} \tag{22}$$

$$k = \begin{cases} \dfrac{\tau_{chem}}{\tau_{chem} + \tau_k} & \text{if } \tau_k > 0 \\ 1 & \text{otherwise} \end{cases}, \tag{23}$$

where ν is the kinematic viscosity and ϵ represents the dissipation rate, while C_{mix} is a constant that can be tuned if needed.

4. Validation test

In order to provide greater reliability to the results obtained, a mesh convergence study was carried out to make the simulation solution independent of the degree of mesh refinement. The simulations performed were non reactive and without injection of lime from the inlet. Only the propeller was put in motion, in order to simulate standard cruise condition of the ship. In addition, a validation of the chemistry model was performed by simulating a 2D reactor in which slaked lime (with an initial concentration of 2 g/l) dissociates, comparing the results obtained with those obtained by Abbate and Bianchi [1]. For the first test, the mesh adopted has been the finest one, constituted by about 16 million cells. Regarding the chemistry validation, the results are compliant with previous data, both in terms of duration of the transient

and stationary values achieved. Results are visible in Figures 3 and 4.

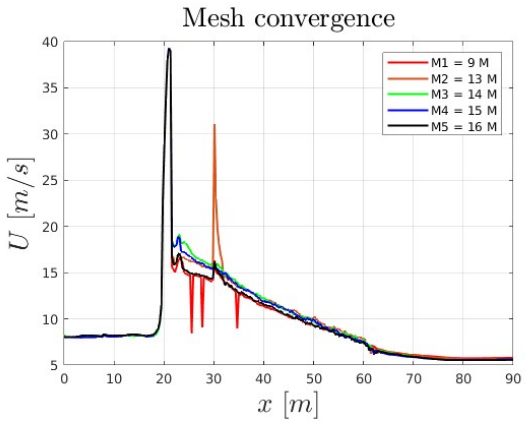

Figure 3: Plot of maximum velocities along the $x-$axis for different mesh sizes, averaged over time.

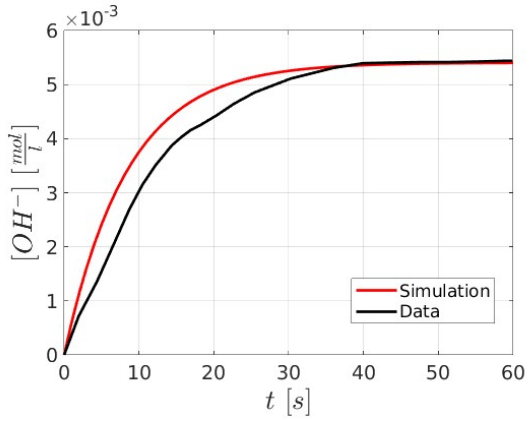

Figure 4: OH^- molar concentrations plotted over time, both for data from Abbate and Bianchi [1] and simulation's results.

5. Results

5.1. Operative Conditions

From Caserini et al. [3], the discharge of rate of slaked lime required in order to attain satisfactory results for deacidification of seawater has been set to $5Kg/s$. Mass flow rates from the inlet and injection velocities change accordingly, and the values, along with other setting parameters, are summarised in the following table.
Other interesting parameters are the temperature and pH of the environment, respectively set to 293 K and 8.2.

	2 g/l	20 g/l	86.5 g/l
Y_{CaOH_2} $[\frac{mol}{l}]$	0.027	0.273	1.169
$\dot{m}_{H_2O}$ $[\frac{l}{s}]$	2500	250	5.78
U_{inlet} $[\frac{m}{s}]$	20	2	0.46

Table 1: Inlet conditions for each case.

5.2. Fluid-dynamic results

From table 1, the 2 g/l case shows a high injection velocity, along with an important flow rate of water from the inlet. For this reason, it's reasonable to assume, and demonstrated by the simulations, that this particular case will affect and influence the flow field, while the other two conditions will differ slightly in terms of velocities and turbulent structures generated. This observations are clearly visible from Figure 5.

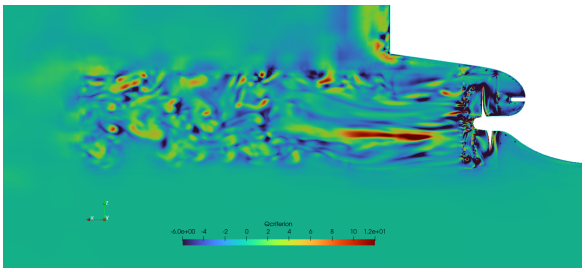

(a)

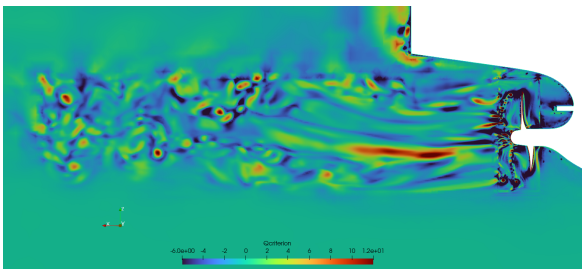

(b)

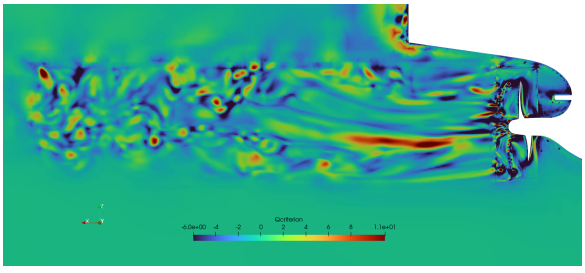

(c)

Figure 5: Comparisons of Q criterion longitudinal slices from 2 g/l (a), 20 g/l (b) and 86 g/l (c) case.

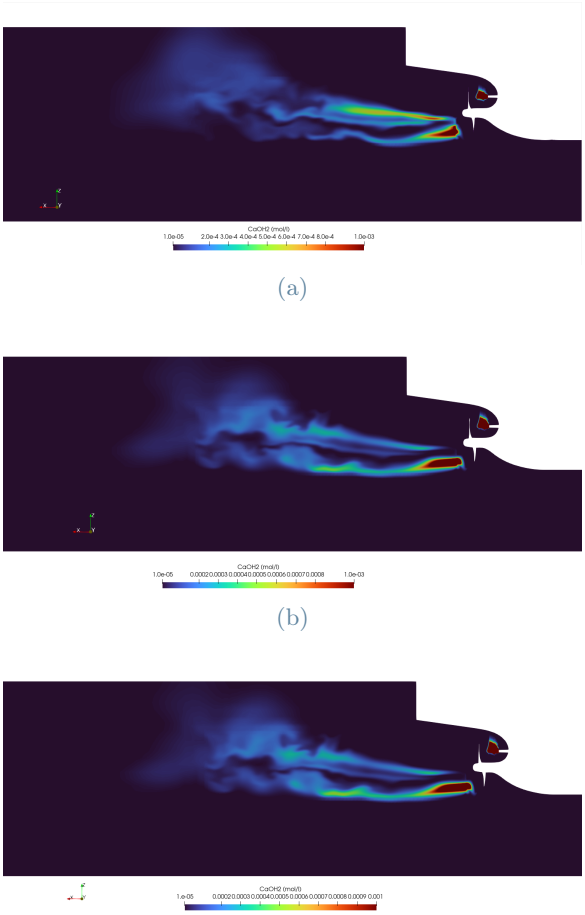

(a)

(b)

(c)

Figure 6: Comparisons of $CaOH_2$ dispersion longitudinal slices from 2 g/l (a), 20 g/l (b) and 86 g/l (c) case.

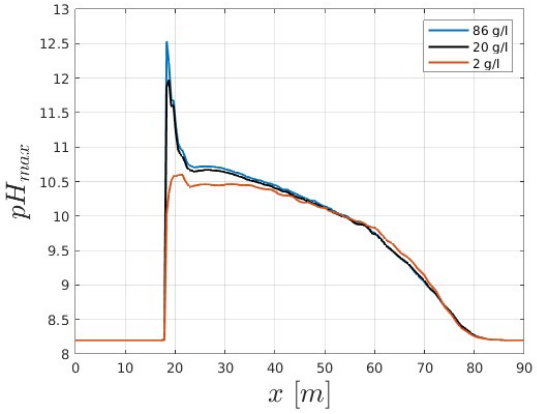

(a)

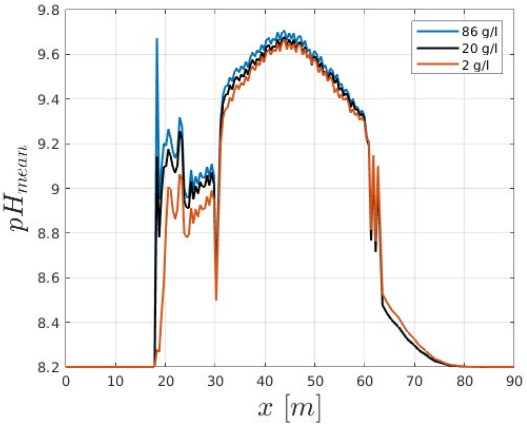

(b)

Figure 7: Maximum (a) and mean (b) pH values for all three cases, along $x-$axis.

The influence of the injection jet is also visible from the slurry dispersion. From Figure 6a, a more concentrated and elongated jet can be appreciated with respect to Figures 6b and 6c, which in contrast show an initial concentrated area of slurry that quickly fades moving away from the propeller, with a pattern almost identical between the two latter conditions.

5.3. Chemistry results

By analyzing the dispersion of OH^- ions, it's possible to plot maximum and mean values, along $x-$axis of pH inside the domain, as plotted in Figure 7. Results are averaged over time, and simulations lasted for 8 seconds. Some observations can be made, shared for both kinds of analysis: the least concentrated case shows no peaks at the injection point, due to the high initial velocity, while the 86 g/l case reach values of pH up to 12.5. After 10 metres from the propeller, the behaviour among the three cases is very similar, returning back to standard values within 60 meters.

The assumption of similar pH diffusion structures can be seen in Figure 8, where contours at fixed pH were compared between cases. The extent and characteristics of the pH clouds are similar except for the 2 g/l case (Figure 8a), which shows some differences due to the influence of the injection jet. Plumes at pH=9 extends similarly for all the three cases simulated, as already confirmed by plots in Figure 7. The maximum distance reached from the propeller is about 60 m, with a maximum width of 14 m. The region with pH=10 (Figure 8b) extends for 53 m in length and 8 m of width. In this visualization it can be appreciated how the 20 and 86.5 g/l cases present iso-surfaces more influenced by the rotating motion of the propeller.

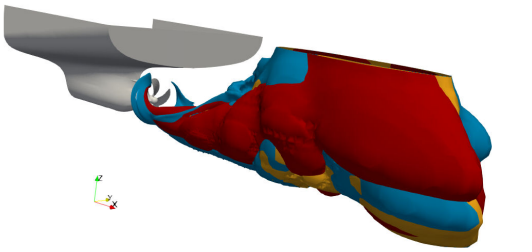

(a)

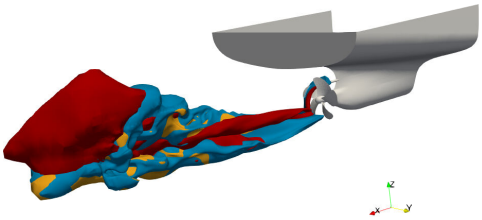

(b)

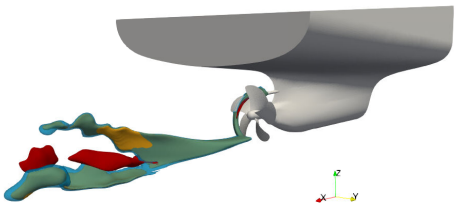

(c)

Figure 8: Comparisons of pH contours between the three cases. (a) represents $pH = 9$, (b) 10, (c) 10.5. 2 g/l contours are red, 20 g/l are yellow, 86 g/l are blue.

In the end, for the pH=10.5 iso-surfaces (Figure 8c), the regions with high pH are significantly less extensive, with thin contours 30 m long for each case.
In conclusion, it should be emphasised that the instability of the phenomenon is a marked characteristic. In fact, analysing the root mean square relative to the calculated time average, it turns out that this reaches deviations of up to 35% in the case of maxima, with a further increase when analysing average values. For the sake of brevity, only the root mean square relative to the maxima are shown in Figure 9.

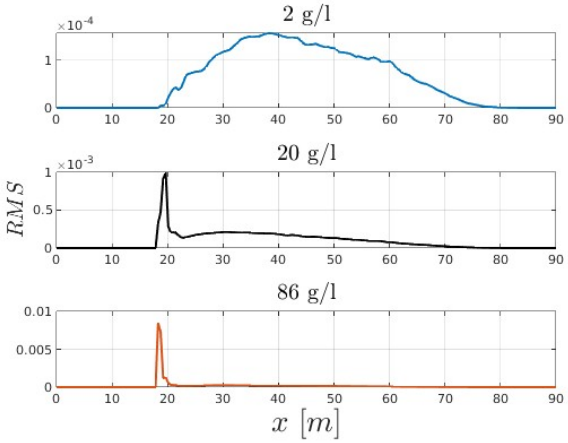

Figure 9: Root mean square of $[OH^-]_{max}$ for each case.

6. Conclusions

In conclusion, a short review of the cases simulated is presented, in order to draw some final observations. The 2 g/l case shows no high peaks of pH, unlike the other two simulations. It is not clear if a pH value of 12.5, even if confined in a very small region, could represent a source of harm for marine biota. All the cases return back to standard values within 60 meters from the injection point. However, the least concentrated case requires large amounts of water, hardly feasible with current ships, thus requiring a readaptation of systems and implants adopted unitl now. From this perspective, 20 and 86 g/l represents a much more practical choice, also given the similar patterns in the second part of the wake.
The tests performed are promising, providing reliable results on the chemical characteristics as well as the fluid dynamics of the problem. However, the analysis could be improved in many aspects, depending on the objective. Sticking with analysing the near-wake zone with an LES approach for the modelling of turbulence, with the improvement of computational resources, the entire domain, or a significantly larger portion, should be simulated with a higher degree of refinement. The unsteadiness of the phenomenon is certainly a problem that needs to be addressed, as can be seen from the RMSs for the $[OH^-]$ concentrations. By simulating for a longer time, thus obtaining more data, it would be possible to increase the degree of confidence in the results obtained. Speaking of the case

with the highest concentration, which must be remembered to be in a saturation condition, in order to provide an adequate term of comparison to results obtained previously (Caserini et al. [3]), it would be appropriate to simulate the solution with a dispersion of molecules within it, as in the physical reality of the problem. In this way, however, it would be necessary to consider more in-depth and detailed chemical kinetics, as well as a more complex particle-flow interaction. These kinds of simulations, known as Lagrangian simulations, can become extremely expensive in terms of computing resources, and certain compromises would have to be made in order to perform a feasible simulation.

7. Acknowledgements

Ringrazio chi mi ha guidato e aiutato lungo questo progetto: la professoressa Antonella Abbà e il professor Federico Piscaglia, così come i ricercatori Simone Abbate e Riccardo Bianchi. Un ringraziamento anche al centro di calcolo CINECA, senza il quale un progetto di queste dimensioni non si sarebbe potuto svolgere.

References

[1] S. Abbate and R. Bianchi. Large eddy simulation of the flow in a stirred tank reactor for calcium hydroxide dissolution. Master's thesis, Politecnico di Milano, 2021.

[2] Nathaniel L. Bindoff, William W. L. Cheung, James G. Kairo, et al. Changing ocean, marine ecosystems, and dependent communities. *IPCC Special Report on the Ocean and Cryosphere in a Changing Climate*, pages 545–546, 2019.

[3] Stefano Caserini, Dario Pagano, Francesco Campo, Antonella Abbà, Serena de Marco, Davide Righi, Phil Renforth, and Mario Grosso. Potential of maritime transport for ocean liming and atmospheric CO2 removal. *Frontiers in Climate*, 2021.

[4] F.Argentieri. A three-dimensional non-reactive fluid dynamics model of the dispersion of calcium hydroxide in the wake of a marine propeller. Master's thesis, Politecnico di Milano, 2020.

[5] M. Germano. A proposal for a redefinition of the turbulent stresses in the filtered navier–stokes equations. *The Physics of Fluids*, 1986.

[6] H.S. Kheshgi. Sequestring atmospheric carbon dioxide by increasing ocean alkalinity. *Energy - The International Journal*, pages 20:915–922, 1995.

[7] KRISO. Kcs ship data: Propeller openwater data. `https://simman2020.kr/download/KCS-Propeller-Openwater-data-KRISO.dat`, accessed 2023-2-2.

[8] J. Smagorinsky. General circulation experiments with the primitive equations. *Monthly Weather Review*, pages 91(3):99–165, 1963.